Int. J. Electrochem. Sci., 14 **(2019)** 2240 – 2245, doi: 10.20964/2019.03.13

International Journal of
ELECTROCHEMICAL
SCIENCE
www.electrochemsci.org

Short Communication

Nickel Oxide Decorated Carbon Nanofibers as High Performance Electrodes for Supercapacitors

Lin Lihua[1,*], *Shi Juanli*[1], *Liao Xiaoqun*[2]

[1] Department of telecommunication and Information Engineering, Xi'an University of Science and Technology, Xi'an 710054, China
[2] Information and Network Center, Xi'an University of Science and Technology, Xi'an 710054, China
[*]E-mail: 407123402@qq.com

Received: 5 November 2018 / *Accepted:* 27 December 2018 / *Published:* 7 February 2019

Hollow carbon nanofibers (HCF) are excellent electrode materials for the supercapacitors in the energy storage area. In this work, hollow carbon nanofibers are prepared firstly. After that, nickel oxide (NiO) nanoparticles are uniformly decorated in HCF (N@HCF) as high performance electrodes for supercapacitors. The electrochemical results indicate that the specific capacity value of N@HCF electrodes is 832 F g^{-1} at the current density of 1 A g^{-1}. Moreover, the N@HCF electrodes show perfect rate performance and superior cycle stability.

Keywords: HCF; N@HCF; Specific Capacity; Electrochemical Performance

1. INTRODUCTION

Energy storage material determines the capacity and energy density of supercapacitors [1, 2]. Therefore, the research on energy storage materials has become an important research topic for the researchers. In order to develop advanced electrode materials, various kinds of materials were studied as electrode for supercapacitors. The electrode materials for supercapacitors can be divided into three categories: carbon materials, conductive polymers and metal oxides [3, 4, 5]. This is because the quality of electrode materials has significant influence on the performance of supercapacitors [6, 7].

A large number of studies have found that the main factors affecting the electrochemical performance of supercapacitors are the specific surface area and pore size distribution of the electrode materials [8, 9, 10]. Among these electrode materials, researchers have done a lot of research in this area. They believe that the capacity value has a linear relationship with the specific surface area of the electrode material [11]. In addition, many teams are conducting research on modification of carbon

materials, such as metal oxide composites [12]. These composite materials can significantly improve the capacity and cycle life of supercapacitors.

In this paper, In this work, hollow carbon nanofibers are prepared firstly. After that, nickel oxide (NiO) nanoparticles are uniformly decorated in HCNF (N@HCF) as high performance electrodes for supercapacitors. The electrochemical results indicate that the specific capacity value of N@HCF electrodes is 832 F g^{-1} at the current density of 1 A g^{-1}. Moreover, the N@HCF electrodes show perfect rate performance and superior cycle stability.

2. EXPERIMENTAL

2.1. Preparation of N@HCF Composites

A red solution of aramid was fabricated by adding 2 g Kevlar 69 and 1 g KOH into dimethyl sulfoxide (DMSO, 200 mL) followed by stirring for 10 days at room temperature [51]. To prepare aramid hydrogels, the as-fabricated aramid solution was frst put in a glass petri dish then deionized water was slowly dropped on top of the aramid solution. Phase segregation started immediately and ANFs hydrogels formed when DMSO was repeatedly exchanged with water. Next, ANFs aerogels were obtained by freeze-drying for 24 h. Finally, to prepare N-doped carbon nanofbers aerogels (NCNAs), the resultant ANFs precursors were pyrolyzed in a tubular furnace under N2 at 1000 °C for 3 h at 5 °C min^{-1} then cooled down naturally. For comparison, the original microfbers of Kevlar 69 were also pyrolyzed under the same conditions as NCNAs, and the obtained sample was designated Kevlar-1000.

2.2. Materials Characterizations

The as-obtained samples were characterized by using transmission electron microscopy (TEM, FEI Tecnai G2 F20), an X-ray diffractometer (XRD, D8 Advance, BRUKER). X-ray photoelectron spectroscopy (XPS) measurements were conducted on XPS-7000 spectrometer. Raman spectra was obtained by Raman Spectrometer (Raman, Advantage 785TM).

2.3. Electrochemical Measurements

The working electrode was prepared by coating the slurry of the active material (20 mg), carbon b lack (2.5 mg), and 60wt% polytetrafluoroethylene (1.6 mL) in small amount of ethanol on Ni foam substrate. Subsequently, the electrodes were dried at 110℃ for 24 h. Electrochemical measurements were conducted on an electrochemical working station (CHI 760E). All electrochemical behaviors of the working electrodes were cyclic voltammetry, galvanostatic charge-discharge, electrical impedance spectroscopy and cycling stability.

3. RESULTS AND DISCUSSION

Figure 1 shows the TEM images of hollow carbon nanofibers and NiO embedded hollow carbon nanofibers composites. As shown in Figure 1a, the as-prepared HCF exhibits hollow carbon structure. Moreover, it can be clearly observed the HCF has mesoporous structure. These mesopores provide hosts for the nickel oxides. Figure 1b displays the TEM image of N@HCF composite. The nickel oxides are uniformly distributed in the mesopores of HCF. This proves that the presence of NiO in the N@HCF composite.

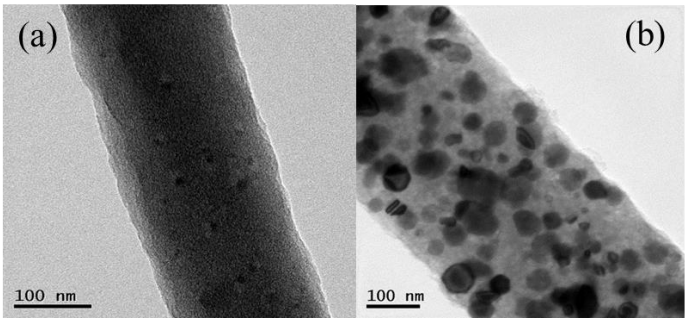

Figure 1. TEM images of (a) HCF, (b) N@HCF composite.

Figure 2a shows the XRD pattern of as-prepared N@HCF composite. As shown in Figure 2a, the typical peaks at the peak positions of 43.5°, 52.9°, 75.7° indicate the presence of metal oxide NiO. These peaks are corresponding to the (111), (200) and (220) planes of NiO [13]. This result confirms the successfully preparation of N@HCF. Figure 2b is the Raman spectra of N@HCF. It can be found that two peaks appeared in the vicinity of 1350 cm^{-1} and 1590 cm^{-1}. The D band centered at 1350 cm^{-1} and G band centered at 1590 cm^{-1} represent for the disordered/defective carbon, and the ordered carbon (sp^2), respectively. The value of I_G/I_D of N@HCF is calculated to be 0.814 according to the fitting curve [14].

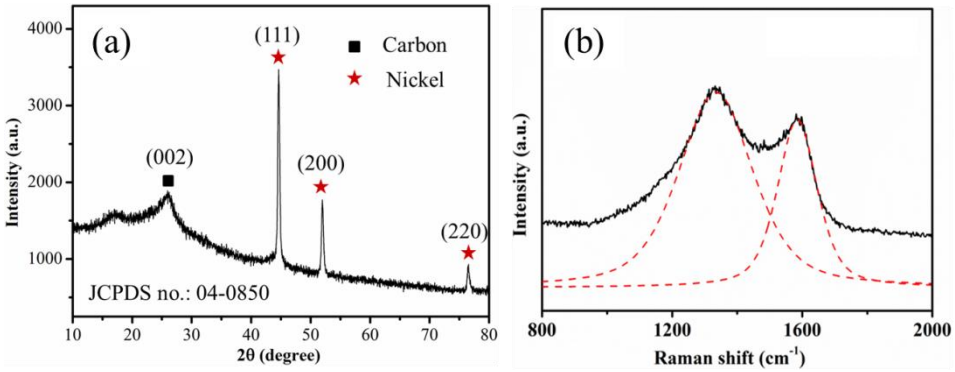

Figure 2. (a) XRD pattern, (b) Raman spectra of N@HCF composite.

To investigate the chemical states in the N@HCF composite, XPS test was applied for the N@HCF composite. In the spectra of C 1s (Figure 3a), the peak at 285.1 ev is corresponding to the C-C/C=C bonding [15]. The Ni 2p shows two main peaks at 163.8, 857 and 169.6 ev, respectively (Figure

3b). This is consistent with Ni $2p_{3/2}$ in the NiO [16]. Furthermore, the XPS test confirms the presence of NiO in the N@HCF composite.

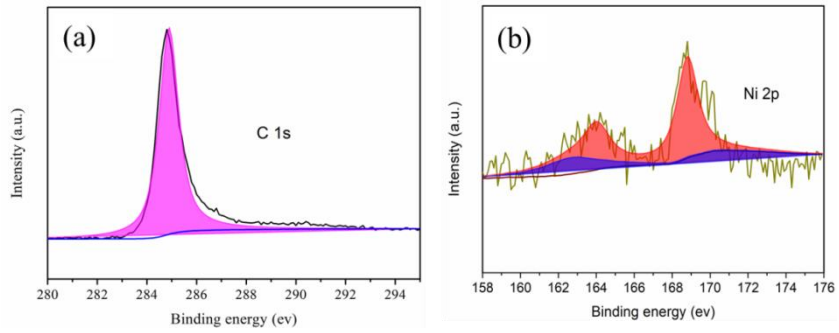

Figure 3. X-ray photoelectron spectroscopy of N@HCF composite.

As shown in Figure 4, the investigations of CV tests on HCF and N@HCF were conducted to evaluate the electrochemical behaviors in 6 M KOH aqueous solution. It can be seen that the N@HCF have redox peaks in the CV curves, indicating pesudocapacitance behavior of surface redox reaction. This is corresponding to the electrochemical reaction as follows [17]:

$$NiO + OH^- \leftrightarrow NiOOH + e^- \quad (1)$$

While the CV curves of HCF show similar rectangle shape, demonstrating typical supercapacitor electrochemical performance. Besides, it can be clearly observed that the N@HCF composite has bigger capacity value than pure HCF electrode.

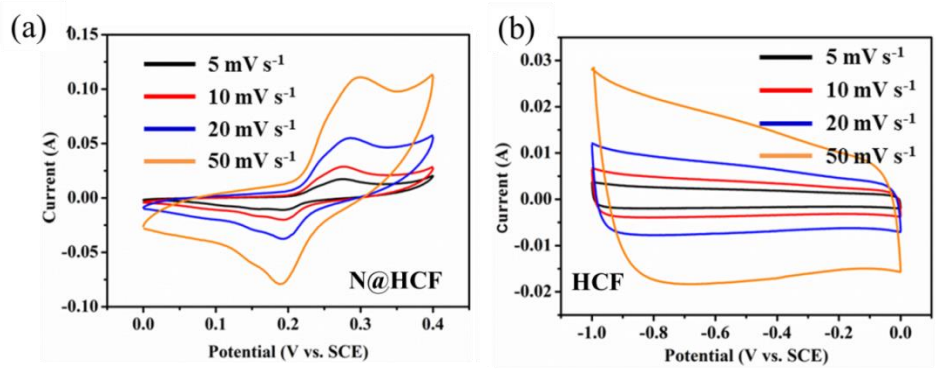

Figure 4. CV curves of (a) N@HCF composite, (b) HCF.

Figure 5 shows discharge curves at different densities from 1 A g^{-1} to 10 A g^{-1}. The specific capacity of the material can be calculated by following formula [18]:

$$C = I\Delta t / m\Delta V \quad (2)$$

"I" represents the current density (A), "△t" is the discharge time (S), "M" is the mass of the active material of the electrode (g), △V is the potential window (V). According to the above formula, it can be seen that under the high current density of 10 A g^{-1}., the specific capacity of N@HCF is 832 F g^{-1}. However, the specific capacity of HCF electrode is only 198 F g^{-1}. More importantly, when the current

densities were improved from 1 A g^{-1} to 10A g^{-1}, the specific capacity value of N@HCF could remain stable. While the specific capacities value of HCF fade rapidly with the improvement of current densities.

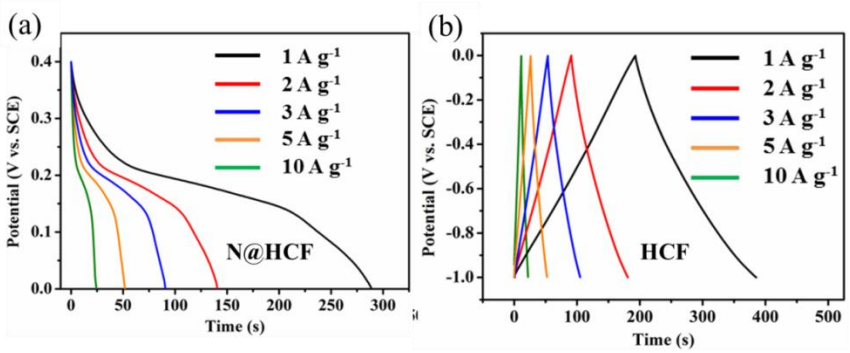

Figure 5. Discharge-charge profiles of (a) N@HCF composite, (b) HCF.

Many literatures have been reported various electrode materials for the high-performance supercapacitors. To clearly demonstrate the excellent electrochemical performance of the as-prepared N@HCF electrode material, the comparison of various electrode materials for supercapacitors is listed in Table 1. It can be seen that the N@HCF electrode shows a capacity value of 832 F g^{-1} even at the high current density of 1 A g^{-1}. This capacity value is much higher than other electrode materials reported in the literatures.

Table 1 The comparison of various electrode materials for supercapacitors.

Electrode	Current Density	Capacity	Reference
N@HCF	1 A g^{-1}	832 F g^{-1}	This Work
HPCR	0.5 A g^{-1}	274 F g^{-1}	19
RAC	1 A g^{-1}	208 F g^{-1}	20
AC	1 A g^{-1}	184 F g^{-1}	21
$Li_4Ti_5O_{12}$/AC	0.5 A g^{-1}	63 F g^{-1}	22

4. CONCLUSIONS

In summary, hollow carbon nanofibers are prepared firstly. After that, nickel oxide nanoparticles are uniformly decorated in HCF (N@HCF) as high performance electrodes for supercapacitors. The electrochemical results indicate that the specific capacity value of N@HCF electrodes is 832 F g^{-1} at the current density of 1 A g^{-1}. Moreover, the N@HCF electrodes show perfect rate performance and superior cycle stability. Therefore, the N@HCF composites would be promising electrode materials for supercapacitors.

ACKNOWLEDGMENT
We thank the financial support from the Xi'an University of Science and Technology.

References

1. C. J. Zhao, Y. X. Huang, C. H. Zhao, X. X. Shao and Z. Q. Zhu, *Electrochim. Acta*, 291 (2018) 287.
2. J. Dominic, T. David, A. Vanaja, G. Muralidharan, N. Maheswari and K. S. Kumar, *Appl. Surf. Sci*., 460 (2018) 40.
3. W. Du, Y. L. Bai, J. Q. Xu, H. B. Zhao, L. Zhang, X. F. Li and J. J. Zhang, *J. Power Sources*, 402 (2018) 281.
4. S. Zhu, J. J. Li, L. Y. Ma, C. N. He, E. Z. Liu, F. He, C. S. Shi and N. Q. Zhao, *Mater. Lett*., 233 (2018) 294.
5. E. Azwar, W. A. Mahari, J. H. Chuah, D. V. Vo, N. L. Ma, W. H. Lam and S. S. Lam, *Int. J. Hydrogen Energ*., 43 (2018) 20811.
6. T. F. Qin, S. L. Peng, J. X. Hao, H. Q. Li, Y. X. Wen, Z. L. Wang, J. J. Huang, F. Ma, J. Hou and G. Z. Cao, *Electrochim. Acta*, 292 (2018) 39.
7. L. Liu, T. Chen, H. Rong and Z. H. Wang, *J. Alloy Copmd*., 766 (2018) 149.
8. M. X. Chen, Y. Yang, D. Z. Chen and H. Wang, *Chinese Chem. Lett*., 29 (2018) 564.
9. J. Xu, J. Q. Li, Q. L. Yang, Y. Xiong and C. G. Chen, *Electrochim. Acta*, 251 (2017) 672.
10. Y. P. Gao, K. J. Huang, H. L. Shuai and L. Liu, *Mater. Lett*., 209 (2017) 319.
11. Q. F. Meng, K. F. Cai, Y. X. Chen and L. D. Chen, *Nano Energ*., 36 (2017) 268.
12. S. Y. Yao, F. Y. Qu, G. Wang and X. Wu, *J. Alloy Compd*., 724 (2017) 695.
13. L. X. Han, Z. F. Xu, J. Wu, X. Q. Guo, H. L. Zhu H. Z. Cui, *J. Alloy Compd*., 729 (2017) 1183.
14. N. N. Bai, Z. Xu, Y. Tian, L. G. Gai, H. H. Jiang, K. L. Marcus and K. Liang, *Electrochim. Acta*, 249 (2017) 360.
15. Y. F. Zhu, H. F. Huang, G. X. Li, X. Q. Liang, W. Z. Zhou, J. Guo, W. L. Wei and S. L. Tang, *Electrochim. Acta*, 248 (2017) 562.
16. J. L. Lv, M. Yang, T. X. Liang and M. Hideo, *Mater. Lett*., 197 (2017) 127.
17. [X. Y. Xu, J. P. Gao, Q. Tian, X. G. Zhai and Y. Liu, *Appl. Surf. Sci*., 411 (2017) 170.
18. F. Li, G. Li, S. Zhang and Y. X. Zhang, *Ceram. Int*., 43 (2017) 8321.
19. L. Fang, Y. P. Xie, Y. Y. Wang, Z. W. Zhang, P. F. Liu, N. Cheng, J. F. Liu, Y. C. Tu, H. B. Zhao and J. J. Zhang, *Appl. Surf. Sci*., 464 (2019) 479.
20. C. J. Zhao, Y. X. Huang, C. H. Zhao, X. X. Shao and Z. Q. Zhu, *Electrochim. Acta*, 291 (2018) 287.
21. C. Wang, J. Wang, W. T. Wu, J. Qian, S. M. Song and Z. B. Yue, *J. Power Sources*, 412 (2019) 683.
22. S. H. Lee and J. M. Kim, *Mater. Lett*., 228 (2018) 220.